Available online at www.sciencedirect.com
ScienceDirect
Journal of Power Sources 163 (2006) 433–439
JOURNAL OF POWER SOURCES
www.elsevier.com/locate/jpowsour

Fabrication and properties of hybrid membranes based on salts of heteropolyacid, zirconium phosphate and polyvinyl alcohol

M. Helen [a], B. Viswanathan [a,*], S. Srinivasa Murthy [b]

[a] *National Centre for Catalysis Research, Department of Chemistry, Indian Institute of Technology, Chennai 600036, India*
[b] *Department of Mechanical Engineering, Indian Institute of Technology, Chennai 600036, India*

Received 13 June 2006; received in revised form 14 August 2006; accepted 15 September 2006
Available online 27 October 2006

Abstract

The fabrication and properties of a hybrid membrane based on cesium salt of heteropoly acid, zirconium phosphate and polyvinyl alcohol are described. The fabricated membranes were characterized for their intra molecular interaction, thermal stability, surface morphology, water content and surface-charge properties using Fourier transform infrared spectroscopy (FTIR), X-ray powder diffraction (XRD), thermogravimetric analysis (TGA), scanning electron microscopy (SEM), water uptake and ion-exchange capacity measurements. These membranes showed reduced methanol crossover (for possible application in DMFC) relative to that of Nafion® 115. At 50% of relative humidity, the protonic conductivity of the hybrid membranes was in the range of 10^{-3} to 10^{-2} S cm^{-1}. The feasibility of these hybrid membranes as proton conducting electrolyte in direct methanol fuel cell (DMFC) was investigated and preliminary results are compared with that of Nafion® 115. A maximum power density of 6 mW cm^{-2} with PVA–ZrP–Cs_2STA hybrid membrane was obtained with the cell operated in passive mode at 373 K and atmospheric pressure. Open circuit voltage of the cell operated with hybrid membranes are high compared to that of Nafion® 115 indicating reduced methanol crossover.

Keywords: Hybrid membrane; Salt of heteropolyacid; Zirconium phosphate; Methanol crossover; Proton conductivity

1. Introduction

The successful performance of a polymer electrolyte membrane fuel cell (PEMFC) critically depends on the role played by the membranes. Nafion®, a perfluorinated ionomer, developed by DuPont, is currently employed in fuel cells though it has limitations like decreased conductivity at low humidity and/or at elevated temperatures, fuel crossover and instability at temperatures of operation higher than 353 K [1–3]. These aspects have prompted research on the design and fabrication of alternative membranes. One such approach is designing membranes based on inorganic organic hybrids [4–12]. This has attracted attention because such hybrids may show controllable thermal, electrical and mechanical properties by virtue of the combination of the properties of organic polymers and inorganic compounds (solid inorganic proton conductors). Solid inorganic proton conductors like zirconium phosphates, heteropolyacids exhibit dual role of being both hydrophilic and proton conducting.

Heteropoly acids (HPAs) are strong Bronsted acids as well as solid electrolytes [13]. For example, hydrated silicotungstic acid ($H_4SiW_{12}O_{40}\cdot 28H_2O$) has an ionic conductivity of 2×10^{-2} S cm^{-1} at room temperature [14–16]. However, HPAs are generally water-soluble. Consequently, a major research objective is to fix the HPAs in stable structure by forming composites [9,17–21] which can maintain their high proton conductivity. Yet another approach in limiting HPAs solubility and leaching is by ion-exchanging protons of HPA with larger cations like Cs^+, NH_4^+, Rb^+ and Tl^+. This aspect has been dealt in detail by Ramani et al. [22,23]. In this work we exploited both these approaches simultaneously by forming composites with polyvinyl alcohol, zirconium phosphate and cesium salt of silicotungstic acid. Water insoluble zirconium phosphate was added to suppress crack formation due to the shrinkage caused during drying. It also contributes to protonic conduction through the proton of phosphate moiety and crystalline water thereby reducing the humidity dependence on conductivity.

* Corresponding author. Tel.: +91 44 22574241; fax: +91 44 22574202.
E-mail address: bvnathan@iitm.ac.in (B. Viswanathan).

0378-7753/$ – see front matter © 2006 Elsevier B.V. All rights reserved.
doi:10.1016/j.jpowsour.2006.09.041

The conductivity of salts of silicotungstic acid was studied [24]. The high protonic conductivity is due to mobile proton that is present as an admixture in the crystalline structure of synthesized salt [25] or due to the presence of crystalline water. The nature of the cation has a great influence on the final properties of the salts of Keggin heteropolyacid. The salts containing small cations, such as Na^+, are soluble in water or in other polar solvents whereas the salts with large cations, such as Cs^+, are insoluble in water [26]. Their low solubility is attributed to the low solvation energy of the large cations. In this paper, the work on a polyvinyl alcohol (PVA) and zirconium phosphate based composite membrane with cesium salts of silicotungstic acid as the active component is described.

2. Experimental

2.1. Materials and membranes preparation

Polyvinyl alcohol (PVA; *M*W: 125,000), silicotungstic acid (SWA) were obtained from SRL Chemicals, orthophosphoric acid (H_3PO_4) was obtained from the E-Merck and zirconium oxychloride ($ZrOCl_2{\cdot}8H_2O$) was obtained from Loba Chemie and were used as received.

2.1.1. Preparation of zirconium phosphate

Zirconium phosphate is prepared by taking 1 M aqueous solution of $ZrOCl_2{\cdot}8H_2O$ and it is slowly added to 10 times excess of 1 M H_3PO_4. The precipitate was washed several times with de-ionized water, dried 2 h at 368 K and stored at 100% RH and room temperature [27].

2.1.2. Synthesis of PVA–ZrP–SWA hybrid membrane

Salts of silicotungstic acid were synthesized at room temperature by neutralization of acid solution with cesium carbonate. Attempts were made to control the number of protons substituted by controlling the stoichiometry of the added cesium carbonate solution. The crystals were dried at room temperature and kept in constant humidity air until constant mass was attained.

A 10% solution of PVA in water was made by constant stirring at 343 K and to that zirconium phosphate (10 wt.%) and cesium salt of silicotungstic acid (30 wt.%) was added and then refluxed the resultant mixture at 343 K for 8 h, to obtain a clear viscous solution. The resulting viscous solution was gelated for 2 days and casted on a clean glass plate with the desired thickness and dried at room temperature to obtain a film.

2.2. Structural characterization

The FTIR (Nicolet 6700 FT-IT using Omnic software) spectra for the samples were recorded in the range 400–4000 cm^{-1} at room temperature. X-ray diffraction patterns were collected with a Rigaku D/max 2400 powder diffractometer using a Cu K_α radiation. The thermogravimetric analysis (TGA) was performed on a Perkin-Elmer TGA (Delta Series TGA 7) instrument at a heating rate of 20 K min^{-1} in air. Scanning electron microscope (FEI, Model: Quanta 200) was used to observe the microstructures of the dried membranes. Elemental analysis of salts of silicotungtic was performed by means of X-ray fluorescence analysis (XRF, Model S4 PIONEER BRUKER aXS) for Cs and W. The composition determined by XRF analysis of the Cs/W atomic ratio, agreed with the composition calculated from the stoichiometric amount of reagents added to prepare Cs salt of silicotungstic acid (Table 1).

Table 1
Cesium content in salts of silicotungtic acid

	Cesium content	
	$Cs_1H_3SiW_{12}O_{40}$	$Cs_2H_2SiW_{12}O_{40}$
Calculated	1	2
XRF analysis	1	1.9

2.3. Water uptake

The water uptake of the hybrid membrane was determined by measuring the change in the weight before and after the hydration. The membrane was first immersed in deionized water for 2 h. Then the membrane was weighed quickly after removing the surface attached water to determine the wetted membrane weight (W_{wet}). The dry membrane weight (W_{dry}) was determined after drying the membrane at 373 K for 2 h.

The water uptake was calculated by using the following equation:

$$\text{Water uptake}\,(\%) = \frac{W_{wet} - W_{dry}}{W_{dry}} \times 100$$

2.4. Swelling

The surface swelling characteristics were determined by measuring the change of the membrane geometrical area upon equilibrating the membranes in water at room temperature for 2 h. The swelling ratio was calculated by the following equation:

$$\text{Swelling}\,(\%) = \frac{A_{wet} - A_{dry}}{A_{dry}} \times 100$$

where A_{dry} and A_{wet} are the area of dry and wet samples, respectively.

2.5. Ion-exchange capacity (IEC)

The ion-exchange capacity of the membranes were determined through an acid–base titration. The dry hybrid membrane was immersed in 50 ml of 1 M sodium chloride aqueous solution for 24 h to exchange protons with sodium ions. The ion-exchanged solution was titrated with 5 mM sodium hydroxide solution using phenolphthalein as an indicator. The ion-exchange capacity was calculated using the following equation:

$$\text{IEC} = \frac{V \times M}{W_{dry}}$$

where IEC is the ion-exchange capacity (meq g^{-1}), V the added titrant volume at the equivalent point (ml), M the molar

concentration of the titrant and W_{dry} is the dry mass of the sample (g).

2.6. Proton conductivity

Proton conductivity was measured by an AC impedance technique (Autolab, PGSTAT 30) using two-probe method, where the AC frequency was scanned from 40 kHz to 10 Hz at voltage amplitude of 5 mV. The proton conductivity (σ) of the samples in the longitudinal direction was calculated from the impedance data, using the relationship $\sigma = d/Rtl$, where d is the distance between the electrodes, t and l the thickness and width of the films, respectively, and R was derived from the low intersect of the high frequency semi-circle on a complex impedance plane with the Re(Z) axis, where Re refers to 'Real' in the complex impedance plane. Prior to the proton conductivity measurements, membranes were immersed in deionised water for 24 h to attain hydration equilibrium. Fully hydrated membranes were sandwiched in a Teflon® conductivity cell equipped with Pt foil contacts and the impedance was measured by placing the cell in a temperature-controlled chamber under a temperature range of 303–373 K. Constant humidity was maintained at 50% RH by using saturated magnesium nitrate [$Mg(NO_3)_2$] and it was sensed by a hygrometer which was calibrated prior to the experiments. The experiments were repeated three times to check the reproducibility. The variation in the results was found to be less than 2%.

2.7. Methanol crossover

Cyclic voltammetric technique was used at room temperature to study the electrochemical reaction of the crossed methanol and to determine its concentrations. For the experiment, a two-compartment glass cell with the membrane separating the two compartments was used. Prior to the measurements, membranes were immersed in deionised water for 24 h to attain hydration equilibrium. Platinum foil with a geometric surface area of 2 cm^2 and smooth platinum electrode were used as working and counter electrode, and Ag/AgCl (saturated KCl) electrode as the reference. The working electrode was immersed in one compartment considered as cathode and counter and reference electrode was immersed in the second compartment considered as anode. The cell was connected to BAS Epsilon potentiostat. Methanol solutions used in this study were prepared with 0.5 M H_2SO_4 electrolyte. The permeability was studied by introducing methanol of known concentration in 0.5 M H_2SO_4 to one compartment of the cell and analyzing the other compartment for its permeability. Prior to the determination of the concentration of the crossed methanol, a blank electrolyte of 50 ml of 0.5 M H_2SO_4 was first added to either compartment of the cell and CV scanning was performed. The permeability test was performed at room temperature for 1 M initial methanol concentration at the anode compartment and cyclic voltomograms of the crossed methanol in the cathode side was plotted between 0.2 and 1 V. The concentration of crossed methanol was determined from the calibration curve which was obtained as described by Ling and Savadogo [28]. The experiments were repeated three times to check the reproducibility. The variation in the results was found to be less than 1.5%.

2.8. MEA fabrication

Electrocatalysts used were unsupported Pt–Ru black (1:1 atomic ratio, Alfa Aesar) and Pt black (Alfa Aesar) in the anode and cathode, respectively. The catalyst slurry containing catalyst, water, isopropyl alcohol (IPA) and Nafion® solution (1100 EW, DuPont) as binder was sprayed on teflonized carbon cloth (E-Tek). Electrode area of 2 cm × 3 cm with 6 mg cm^{-2} of catalyst loading were fabricated and placed on either side of the membrane. The membrane electrode assembly (MEA) was sandwiched between the two transparent polyacrylic plates constituting the cell fixture by means of six bolts. Single cell performance was measured by using a passive DMFC with a 4 M methanol solution. Methanol was diffused into the anode catalyst layer from the built-in reservoir of 4.5 ml capacity, while oxygen, from the surrounding air, was diffused into the cathode catalyst layer through the opening of the cathode fixture. The single cell performance experiments were carried out at room temperature (273 K) and at atmospheric pressure. Cell voltage versus current density response was measured galvanostatically by incrementally increasing the current from open circuit and measuring the cell voltage.

3. Results and discussion

3.1. FTIR spectroscopy

The FTIR spectra of PVA–ZrP–Cs_1SWA and PVA–ZrP–Cs_2SWA membranes obtained are shown in Fig. 1. The spectrum of a typical membrane reveals the characteristic bands of PVA, α-ZrP and salt of SWA. The FTIR spectrum of hybrid membranes showed bands at 981, 917, 876 and 790 cm^{-1}, which agree with those reported in literature [29,30] for this silicotungstic acid. The same characteristic bands are seen in the hybrid membrane containing salts of silicotungstic acid. The band at 981 cm^{-1} corresponds to the stretching of the W=O_t terminal bond and the band at 917 cm^{-1} corresponds to the stretching of X–O bond which is red shifted from 926 cm^{-1}, this is due to the columbic interaction between the hydroxyl groups of the polyvinyl alcohol donor and the salt of silicotungstic acid in the hybrid membrane. The bands at 876 and 793 cm^{-1} corresponds to the W–O_b–W (O_b-bridged oxygen and O_t-terminal oxygen) connecting two [W_3O_{13}] units by corner sharing and by edge sharing, respectively. The later has blue shifted from 779 to 793 cm^{-1} which again represents the columbic interaction. The bands at 3260 and 2907 cm^{-1} represents O–H stretching and –CH_2 stretching; the band around 1420 cm^{-1} is for –CH_3 bending which are characteristic of PVA. The bands around 510 and 1050 cm^{-1} are due to Zr–O and P–O_4 symmetric stretching and that around 916 cm^{-1} is due to P–OH asymmetric stretching which are characteristics of ZrP. The main bands are assigned and tabulated separately for PVA–ZrP–Cs_1STA and PVA–ZrP–Cs_2STA hybrid membranes in Table 2.

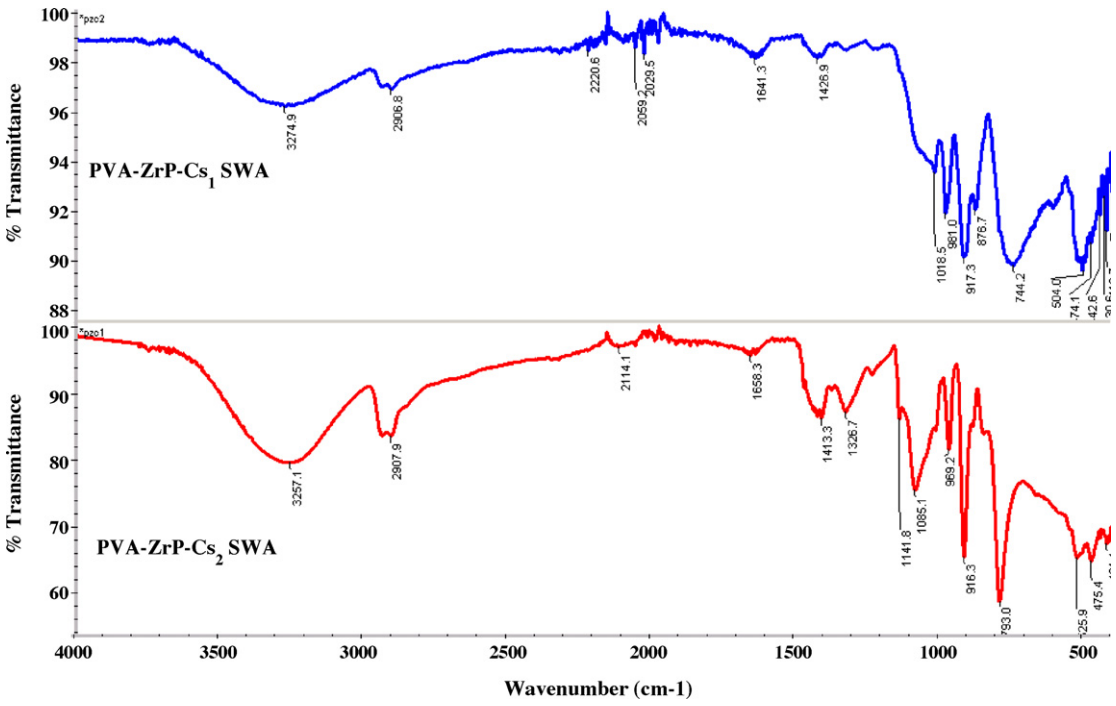

Fig. 1. FTIR spectra of PVA–ZrP–Cs_1SWA and PVA–ZrP–Cs_2SWA hybrid membranes.

3.2. XRD

X-ray diffractograms of PVA–ZrP–Cs_1STA and PVA–ZrP–Cs_2STA hybrid membranes are shown in Fig. 2. All the indexed peaks are due to Cs salt of silicotungtic acid and are indexed according to the JCPDS card no. 51-0416. The broad hump in the 2θ range 20–35 is due to the presence of PVA and zirconium phosphate.

Table 2
Assignments of main absorption bands for PVA–ZrP–Cs_1SWA and PVA–ZrP–Cs_2SWA hybrid membranes

Vibration frequency (cm^{-1})		Bond assignment
PVA–ZrP–Cs_1SWA	PVA–ZrP–Cs_2SWA	
981	969	W═O_t stretching
917	916	X─O stretching
876	–	Corner sharing W─O_b─W
744	793	Edge sharing W─O_b─W
3274	3257	O─H stretching
2906	2907	─CH_2 stretching
1426	1413	─CH_3 bending
504	525	Zr─O symmetric stretching
1018	1085	P─O_4 symmetric stretching

Table 3
Water uptake, swelling and IEC values for PVA–ZrP–Cs_1SWA and PVA–ZrP–Cs_2SWA hybrid membranes with a 180 μm thickness compared with Nafion® 115

Membrane	Water uptake (%)	Swelling (%)	IEC (meq g^{-1})
PVA–ZrP–Cs_1SWA	260	100	3.2
PVA–ZrP–Cs_2SWA	140	85	3
Nafion® 115	22	12	0.9

3.3. Thermal analysis

Fig. 3 illustrates the thermogravimetric analysis of the hybrid membranes in the temperature range from 323 to 1073 K. Three degradation stages are seen, the first weight loss occurred at temperatures around 373 K, was associated with the loss of absorbed water molecules and a major second weight loss is due to decomposition of polyvinyl alcohol in the temperature region 473–573 K and the loss of crystalline water from silicotungstic acid. The third major weight loss is due to decomposition of salt of silicotungstic acid to respective metal oxides combined with

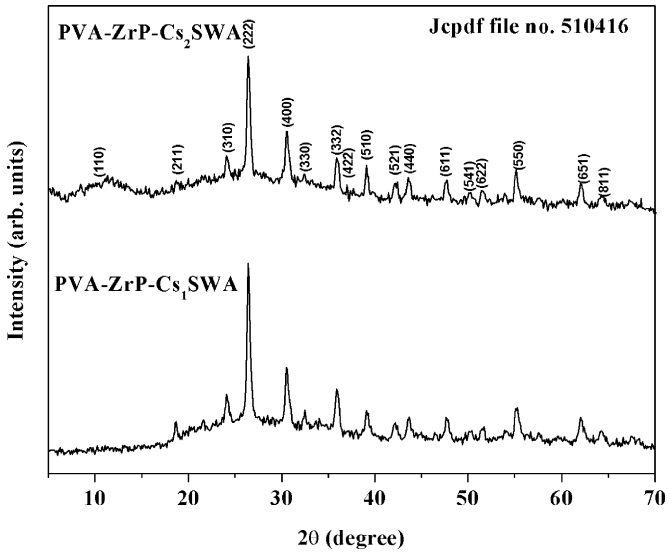

Fig. 2. Cu K_α XRD patterns of PVA–ZrP–Cs_1SWA and PVA–ZrP–Cs_2SWA hybrid membranes and its components for comparison.

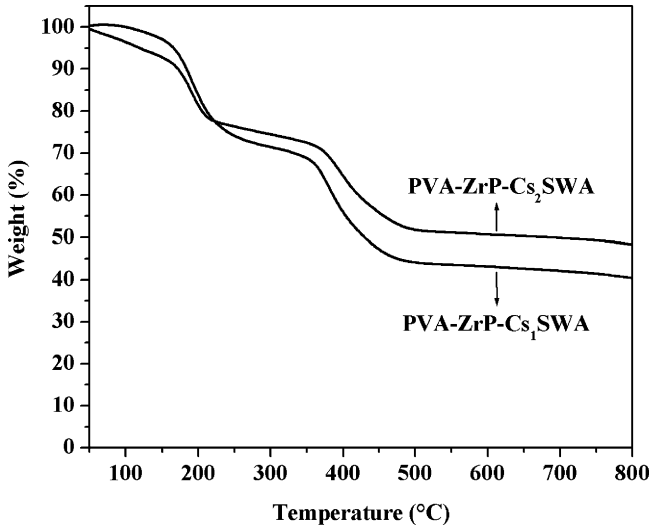

Fig. 3. TGA analysis of PVA–ZrP–Cs_1SWA and PVA–ZrP–Cs_2SWA hybrid membranes in a temperature range from 50 to 800 °C.

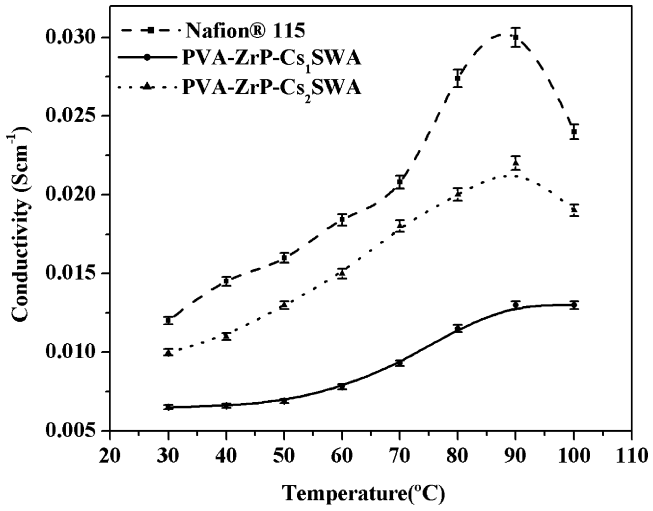

Fig. 5. Proton conductivity at 50% RH as a function of temperature for PVA–ZrP–Cs_1SWA and PVA–ZrP–Cs_2SWA membranes compared with Nafion® 115 at 100% RH.

the loss associated with the phase transition of ZrP to nonlayered pyrophosphate (ZrP_2O_7) phase.

3.4. SEM

Surface morphology of the dried membrane was investigated using SEM. Fig. 4 shows the scanning electron micrographs of PVA–ZrP–Cs_1SWA and PVA–ZrP–Cs_2SWA hybrid membranes. The distribution of inorganic particles is relatively uniform in the organic matrix. Membranes are compact with no phase separation suggesting that the synthesized films were homogeneous in nature and hence formed dense membrane.

3.5. Water uptake, swelling and IEC

Water uptake and ion-exchange capacity of the membrane plays an important role in conductivity. Presence of water greatly influences the basic properties of the membrane. With increase

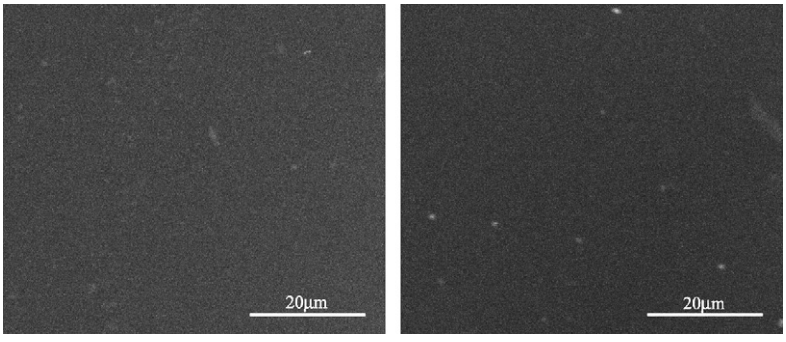

Fig. 4. Scanning electron micrographs of PVA–ZrP–Cs_1SWA and PVA–ZrP–Cs_2SWA hybrid membranes.

Table 4
Comparison of conductivity and permeability for various membranes

Membrane	Relative humidity (%)	Temperature (°C)	Conductivity (S cm^{-1})	Permeability (cm^2 s^{-1})	Reference
PVA–ZrP–Cs_1SWA	50	100	0.013	2×10^{-6}	[a]
PVA–ZrP–Cs_2SWA	50	100	0.02	3×10^{-6}	[a]
Nafion® 115	100	90	0.03	3.5×10^{-6}	[a]
Nafion® 115/Cs^+, NH_4^+, Rb^+ and Tl^+ modified PTA	35	120	0.016	–	[21]
SPEK/ZP/ZrO_2 (70/20/10 wt.%)	100	70	2.3×10^{-3}	–	[11]
PVA/PWA/SiO_2	–	–	0.004–0.017	10^{-7} to 10^{-8}	[12]
PEG/SiO_2/SWA	100	80	0.01	10^{-5} to10^{-6}	[7]
PEG/SiO_2/PWA	–	–	10^{-5} to 10^{-3}	10^{-6} to10^{-7}	[20]
PVA–SiO_2–SWA	100	100	4.13×10^{-3}	–	[9]
SPEEK/PWA	100	100	1.7×10^{-2}	–	[19]

[a] Obtained from our measurements.

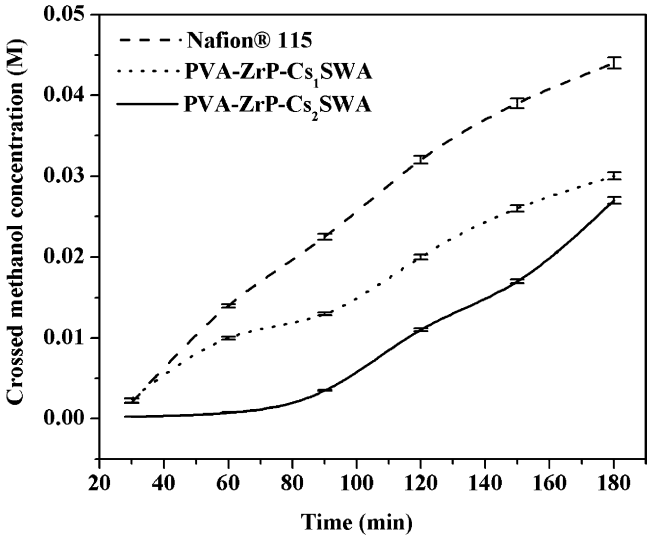

Fig. 6. Concentration of crossed methanol as a function of crossover time.

in water uptake and IEC, proton conductivity increases due to increase in the mobility of ions in the water phase. The water uptake, swelling and IEC data for the membranes are given in Table 3. At room temperature the water absorption and swelling decrease with increase in cesium content for membranes of 180 μm thickness.

3.6. Proton conductivity

Fig. 5 shows temperature dependence of the membrane conductivity. At 50% of relative humidity, the protonic conductivity of the hybrid membranes was in the range of 10^{-3} to 10^{-2} S cm^{-1}. The proton conductivity increased with increasing substitution of proton with cesium. The charge carriers in the acidic salt of silicotungstic acid are increasing leading to increased proton conductivity in PVA–ZrP–Cs_2SWA compared to PVA–ZrP–Cs_1SWA hybrid membrane [24]. Proton conductivity is steadily increasing with temperature for both the hybrid membranes and for comparison the corresponding data for Nafion® 115 measured at 100% relative humidity are included in Fig. 5.

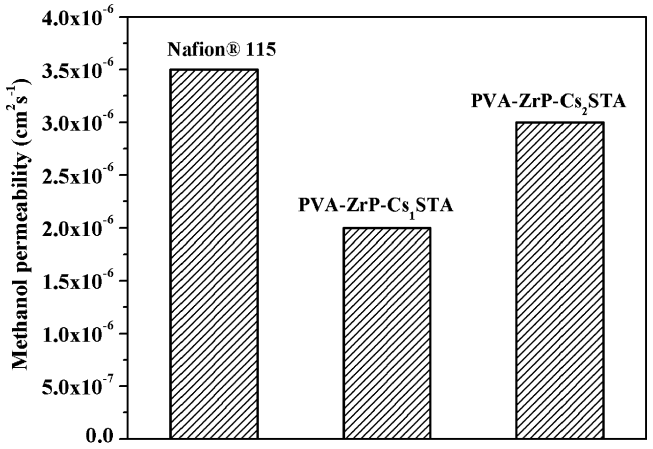

Fig. 7. Methanol permeability of PVA–ZrP–Cs_1SWA and PVA–ZrP–Cs_2SWA hybrid membranes compared with Nafion® 115.

3.7. Methanol crossover

The concentration of crossed methanol as a function of crossover time is determined for PVA–ZrP–Cs_1STA and

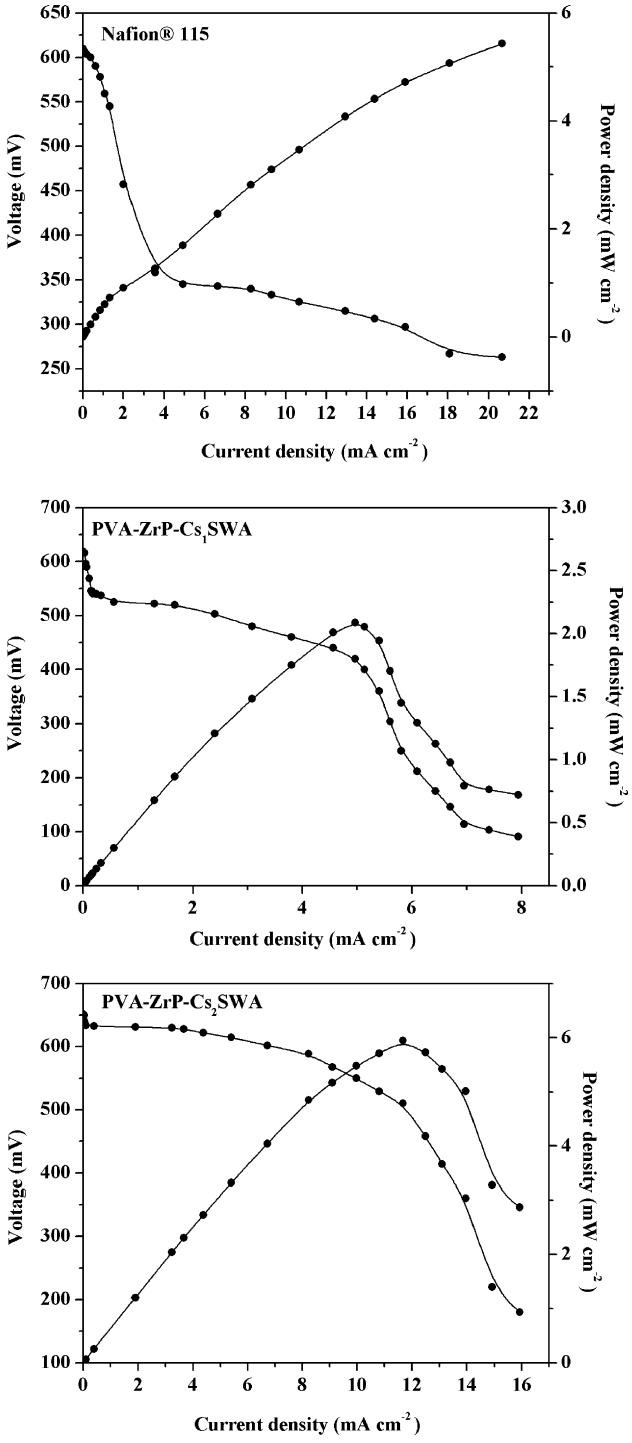

Fig. 8. Polarization and power density curves for passive DMFC cell with Nafion® 115, PVA–ZrP–Cs_1SWA and PVA–ZrP–Cs_2SWA hybrid membranes as proton conducting electrolyte at 273 K and at atmospheric pressure.

PVA–ZrP–Cs_2STA hybrid membranes and it is compared to Nafion® 115 in Fig. 6. At 180 min the methanol crossed over in hybrid membranes is 33% less compared to Nafion® 115. In the case of hybrid membranes there is an exponential increase in crossover whereas in the case of Nafion® 115 it is linear with respect to crossover time. Among the two hybrid membranes PVA–ZrP–Cs_2STA shows lesser crossover to methanol. As shown in Fig. 7, the methanol permeability for hybrid membranes was less compared to Nafion® 115. Compared to Nafion® 115 and other related membranes, hybrid membranes containing cesium salt of SWA show resistance to methanol permeability with appreciable proton conductivity as shown in Table 4.

3.8. Single cell performance in DMFC

Fig. 8 shows the single cell performance of DMFC with PVA–ZrP–Cs_1STA and PVA–ZrP–Cs_2STA hybrid membranes as proton conducting electrolyte. For comparison, the single cell performance of Nafion® 115 as proton conducting electrolyte under similar condition is also shown. The polarization and power density curves are obtained under unoptimized conditions by a home made passive cell. Cell with PVA–ZrP–Cs_2STA hybrid membrane delivers a maximum power density of 6 mW cm^{-2} which is comparable to that of Nafion® 115 (5.4 mW cm^{-2}). The cell with PVA–ZrP–Cs_1STA hybrid membrane exhibited lower performance (2.1 mW cm^{-2}) in full cell mode in comparison to PVA–ZrP–Cs_2STA hybrid membrane and Nafion® 115. The open circuit voltage (OCV) for the cell with PVA–ZrP–Cs_2STA hybrid membrane is 0.652 V and that for PVA–ZrP–Cs_1STA hybrid membrane is 0.619 V. The increase in OCV compared to Nafion® 115 (0.610 V) indicated reduced methanol crossover to the cathode side. The results suggest that these membranes may be suitable for application in DMFC.

4. Conclusion

Though number of reports are available in literature on stabilizing the HPA in membrane matrix, a combined approach of composite formation with salts of HPA was investigated. Hybrid membranes based on cesium salt of heteropoly acid, zirconium phosphate and polyvinyl alcohol were fabricated and characterized for its applicability in DMFC. The vibration spectroscopy, diffraction studies and thermal analysis provided information on the structure and stability of these hybrid membranes. Water uptake and swelling of the fabricated membranes decreased with increase in cesium content. At 50% of relative humidity, the protonic conductivity of the hybrid membranes was in the range of 10^{-3} to 10^{-2} S cm^{-1}. Also, these hybrid membranes exhibited decreased methanol crossover with that of Nafion® 115. A maximum power density of 6 mW cm^{-2} was obtained with PVA–ZrP–Cs_2STA hybrid membrane. The open circuit voltage for the cell with PVA–ZrP–Cs_2STA hybrid membrane is 0.652 V and that for PVA–ZrP–Cs_1STA hybrid membrane is 0.619 V which is higher compared to the cell with Nafion® 115 (0.610 V) indicating reduced methanol crossover. The performance of the hybrid membranes in passive cell mode was found to be most promising for DMFC applications.

Acknowledgments

The authors wish to record their gratefulness to the Department of Science and Technology for the support to create the National Centre for Catalysis Research (NCCR) at the Indian Institute of Technology, Madras. The funding by Ms. Columbian Chemicals Company, Georgia is also gratefully acknowledged.

References

[1] J.J. Sumner, S.E. Creager, J.J. Ma, D.D. Desmarteau, J. Electrochem. Soc. 145 (1998) 107–110.
[2] J. St-Pierre, D.P. Wilkinson, AIChE J. 47 (1998) 1482–1486.
[3] S. Slade, S.A. Campbell, T.R. Ralph, F.C. Walsh, J. Electrochem. Soc. 149 (2002) A1556–A1564.
[4] T. Tezuka, K. Tadanaga, A. Matsuda, A. Hayashi, M. Tatsumisago, Solid State Ionics 176 (2005) 3001–3004.
[5] S. Li, Z. Zhou, M. Liu, W. Li, J. Ukai, K. Hase, M. Nakanishi, Electrochim. Acta 51 (2006) 1351–1358.
[6] P.G. Romero, J.A. Asensio, S. Borrós, Electrochim. Acta 50 (2005) 4715–4720.
[7] D.R. Vernon, F. Meng, S.F. Dec, D.L. Williamson, J.A. Turner, A.M. Herring, J. Power Sources 139 (2005) 141–151.
[8] D.S. Kim, H.B. Park, J.W. Rhim, Y.M. Lee, J. Membr. Sci. 240 (2004) 37–48.
[9] S. Shanmugam, B. Viswanathan, T.K. Varadarajan, J. Membr. Sci. 275 (2006) 105–109.
[10] S. Panero, P. Fiorenza, M.A. Navarra, J. Romanowska, B. Scrosati, J. Electrochem. Soc. 152 (2005) A2400–A2405.
[11] B. Ruffmann, H. Silva, B. Schulte, S.P. Nunes, Solid State Ionics 162–163 (2003) 269–275.
[12] W. Xu, C. Liu, X. Xue, Y. Su, Y. Lv, W. Xing, T. Lu, Solid State Ionics 171 (2004) 121–127.
[13] M. Misono, Catal. Rev. Sci. Eng. 29 (1987) 269321.
[14] O. Nakamura, T. Kodama, I. Ogino, Y. Miyake, Chem. Lett. 1 (1979) 17–18.
[15] O. Nakamura, I. Ogino, T. Kodama, Solid State Ionics 3–4 (1981) 347–351.
[16] K.-D. Kreuer, J. Mol. Struct. 177 (1988) 265–276.
[17] P. Staiti, J. New Mater. Electrochem. Syst. 4 (2001) 181–186.
[18] B. Tazi, O. Savadogo, Electrochim. Acta 45 (2000) 4329–4339.
[19] S.M.J. Zaidi, S.D. Mikhailenko, G.P. Robertson, M.D. Guiver, S. Kaliaguine, J. Membr. Sci. 173 (2000) 17–34.
[20] C.W. Lin, R. Thangamuthu, P.H. Chang, J. Membr. Sci. 254 (2005) 197–205.
[21] M.L. Ponce, L. Prado, B. Ruffman, K. Richau, R. Mohr, S.R. Nunes, J. Membr. Sci. 217 (2003) 5.
[22] V. Ramani, H.R. Kunz, J.M. Fenton, Electrochim. Acta 50 (2005) 1181–1187.
[23] V. Ramani, H.R. Kunz, J.M. Fenton, J. Power Sources 152 (2005) 182–188.
[24] A. Vakulenko, Y. Dobrovolsky, L. Leonova, A. Karelin, A. Kolesnikova, N. Bukun, Solid State Ionics 136–137 (2000) 285–290.
[25] V. Shteinberg, B. Shumm, L. Erofeev, A. Korosteleva, L. Leonova, E. Ukshe, Fiz. Tverdogo Tela 31 (1989) 128–132.
[26] M.A. Parent, J.B. Moffat, J. Catal. 177 (1998) 335–342.
[27] F. Bauer, M.W. Porada, J. Power Sources 145 (2005) 101–107.
[28] J. Ling, O. Savadogo, J. Electrochem. Soc. 151 (2004) A1604.
[29] T. Okuhara, N. Mizuno, M. Misono, Adv. Catal. 41 (1996) 113–252.
[30] C. Rocchiccioli-Deltcheff, R. Thouvenot, R. Franck, Spectrochim. Acta A 32 (1976) 587–597.